Axion detection in the 10^{-4} eV mass range

Pierre Sikivie, D. B. Tanner, and Yun Wang*
Physics Department, University of Florida, Gainesville, Florida 32611
(Received 11 May 1994)

We propose an experimental scheme to search for galactic halo axions with mass $m_a \sim 10^{-4}$ eV, which is above the range accessible with cavity techniques. The detector consists of a large number of parallel superconducting wires embedded in a material transparent to microwave radiation. The wires carry a current configuration which produces a static, inhomogeneous magnetic field $\mathbf{B}(\mathbf{x})$ within the detector volume. Axions which enter this volume may convert to photons. We discuss the feasibility of the detector and its sensitivity.

PACS number(s): 95.35.+d, 14.80.Mz

The axion has remained a prime candidate for dark matter [1]. Current constraints on the axion allow masses between 10^{-3} and 10^{-7} eV. If the galactic halo is made up exclusively of axions, their density in the solar neighborhood is approximately 0.5×10^{-24} g/cm^3 and their velocity dispersion is approximately $10^{-3}c$. Galactic halo axions can be detected by stimulating their conversion to photons in an electromagnetic cavity permeated by a strong magnetic field [2]; detectors of this type are being built with increasing sensitivity [3]. However, at the present time, it appears that these cavity detectors cannot cover the entire mass window. In particular, their range is limited in the direction of large axion masses by the complexities involved in segmenting a given magnetic volume into many small cavities. The most complex system envisaged so far would reach $m_a \simeq 1.6\times10^{-5}$ eV [3]. Much larger masses are difficult for the cavity detector to access given presently available technology. In this paper, elaborating on earlier ideas [4], we propose an alternative approach which is specifically intended to address the possibility of larger axion masses.

The basis for the detector is as follows. The coupling of the axion to two photons is [1] ($\hbar = c = 1$)

$$\mathcal{L}_{a\gamma\gamma} = \frac{\alpha}{8\pi}\frac{a}{f_a}\left[\frac{N_e}{N} - \left(\frac{5}{3} + \frac{m_d - m_u}{m_d + m_u}\right)\right] F_{\mu\nu}\tilde{F}^{\mu\nu} \equiv \frac{\alpha}{4\pi}\frac{a}{f_a} g_\gamma F_{\mu\nu}\tilde{F}^{\mu\nu} , \quad (1)$$

where α is the fine structure constant, a is the axion field, f_a is the axion decay constant, m_u and m_d are the up and down quark current masses, and N and N_e are model-dependent coefficients. In grand unified axion models, one has $N_e/N = \frac{8}{3}$, and hence $g_\gamma = m_u/(m_u + m_d) \simeq 0.36$. The axion mass is given by

$$m_a = \frac{f_\pi m_\pi}{f_a}\frac{\sqrt{m_u m_d}}{m_u + m_d} \simeq 0.6 \text{ eV}\left(\frac{10^7 \text{ GeV}}{f_a}\right) . \quad (2)$$

Thus Eq. (1) can be rewritten

$$\mathcal{L}_{a\gamma\gamma} = -g_\gamma \frac{\alpha}{\pi}\frac{m_a}{0.6\times10^{16}\ (\text{eV})^2} a\mathbf{E}\cdot\mathbf{B} . \quad (3)$$

Because of the coupling of Eq. (1), axions will convert to photons (and vice versa) in an externally applied magnetic field. The cross section for $a \to \gamma$ conversion in a region of volume V and dielectric constant ϵ and permeated by a static magnetic field $\mathbf{B}(\mathbf{x})$ is [2]

$$\sigma = \frac{1}{16\pi^2\beta_a}\left(\frac{\alpha g_\gamma}{\pi f_a}\right)^2 \frac{1}{\epsilon}\int d^3k_\gamma \delta(E_a - \omega) \times \left|\int_V d^3x\, e^{i(\mathbf{k}_\gamma - \mathbf{k}_a)\cdot\mathbf{x}} \mathbf{n}\times\mathbf{B}(\mathbf{x})\right|^2 , \quad (4)$$

where $(E_a, \mathbf{k}_a) = E_a(1, \boldsymbol{\beta}_a)$ is the axion four-momentum, and $(\omega, \mathbf{k}_\gamma) = \omega(1, \sqrt{\epsilon}\mathbf{n})$ is the photon four-momentum. $\mathbf{n}$ is the unit vector in the direction of $\mathbf{k}_\gamma$. $E_a = \omega$ because the magnetic field is static. The momentum transfer $\mathbf{q} = \mathbf{k}_\gamma - \mathbf{k}_a$, which is necessary because the photon is massless while the axion is massive, is provided by the inhomogeneity of the magnetic field. Galactic halo axions are nonrelativistic, with $k_a \sim 10^{-3}m_a$. Hence, to obtain resonant conversion the magnetic field should be made inhomogeneous on the length scale $(m_a\sqrt{\epsilon})^{-1}$.

Figure 1 shows schematic top and side views of the detector we propose. It consists of an array of parallel superconducting wires embedded in a microwave-transparent dielectric. The dielectric medium keeps the wires in place. The dimensions of the detector are (L_x, L_y, L_x). $\hat{\mathbf{y}}$ is the common direction of the wires. The intersections of the wires with the (x, z) plane form an array with unit cell size $d \lesssim m_a^{-1}$. We denote the location of a wire with the integers (n_z, n_x) where

$$n_x \in (-N_x/2, N_x/2), \quad N_x d = L_z ,$$

$$n_x \in (-N_x/2, N_x/2), \quad N_x d = L_x .$$

Let the wires carry the following current configuration:

$$I(n_z, n_x) = I(n_z) = I_0 \sin(n_z dq) . \quad (5)$$

In the limit $L \to \infty$ and $d \to 0$, the magnetic field generated is $\mathbf{B}(z) = -\hat{\mathbf{x}}B_0\cos(qz)$ where $B_0 = I_0/(qd^2)$.

*Present address: NASA/Fermilab Astrophysics Center, FNAL, Batavia, IL 60510-0500.

Resonant conversion occurs when $q \sim \sqrt{\epsilon} m_a$.

We expect the magnetic field to be dominated by the $\mathbf{B}(z) = -\hat{\mathbf{x}} B_0 \cos(qz)$ term but, since our detector has finite volume, the field is modified by finite size effects. We discuss these now. The $\hat{\mathbf{x}}$ component of the magnetic field at point (z, x) inside the detector is given by

$$B_x(z,x) = \frac{I_0}{2\pi} \sum_{n_z=-N_z/2}^{N_z/2} \sin(qdn_z) \times \sum_{n_x=-N_x/2}^{N_x/2} \frac{z - n_z d}{(z-n_z d)^2 + (x - n_x d)^2} \,. \quad (6)$$

Replacing sums with integrals, we find

$$B_x(z,x) \simeq -B_0 \left[f(x) \cos(qz) - \tfrac{1}{2} g(x,z) \cos\left(\frac{gL_z}{2}\right) + O\left(\frac{1}{qL}\right) \right] , \quad (7)$$

for $|x| \le L_x/2$ and $|z| \le L_z/2$, where

$$\begin{aligned} B_0 &\equiv \frac{I_0}{qd^2} \,, \\ f(x) &\equiv 1 - e^{-qL_x/2} \cosh(qx) \,, \\ g(x,z) &\equiv \frac{1}{\pi} \left[\arctan\left(\frac{L_x/2 - x}{L_z/2 - z}\right) + \arctan\left(\frac{L_x/2 - x}{L_z/2 + z}\right) + \arctan\left(\frac{L_x/2 + x}{L_z/2 - z}\right) + \arctan\left(\frac{L_x/2 + x}{L_z/2 + z}\right) \right] . \end{aligned} \quad (8)$$

Note that $f(x) = 1$ everywhere inside the detector volume, except within a distance $\Delta x \sim q^{-1} \sim m_q^{-1}$ from the surface. Equation (7) shows that the most important finite size effects occur when $\cos(qL_z/2) \neq 0$. Figure 2 shows the x dependence of B_x when $|\cos(qL_z/2)| = 1$, which is when the finite size effects are largest. Both the exact [Eq. (6)] and the approximate [Eq. (7)] expressions for B_x are plotted. There is excellent agreement between the two. Of course, the exact curve displays the kinks in B_x which result from the discreteness of the current distribution, whereas the other curve is smooth.

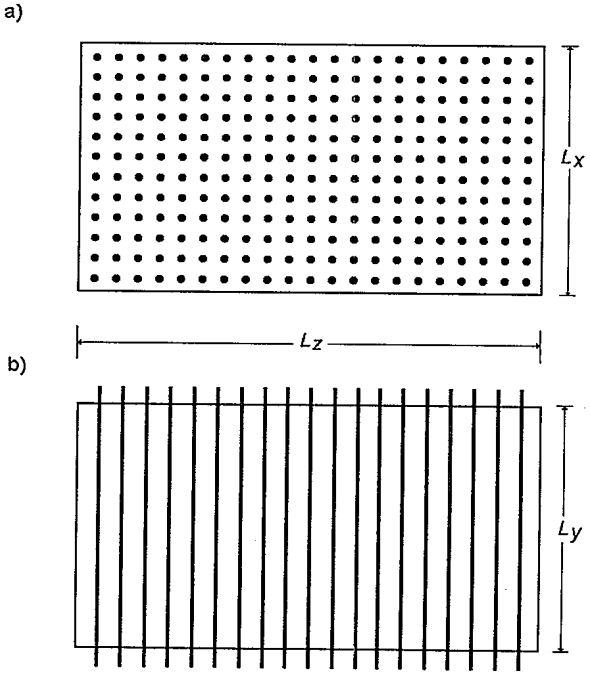

FIG. 1. Top and side views of the detector, showing the arrangement of wires.

Henceforth, we will make the simplifying assumption that $\mathbf{B} = \hat{\mathbf{x}} B_x(z)$. For $m_a L_x$, $m_a L_y \gg 1$, Eq. (4) becomes

$$\sigma = \sigma_0 \sum_{n_z=\pm 1} \left| \frac{1}{L_z} \int_{-L_z/2}^{L_z/2} dz \frac{B_x(z)}{B_0} e^{iE_a(n_z\sqrt{\epsilon} - \beta_{az})z} \right|^2 , \quad (9)$$

where we have dropped terms of $O(\beta_a^2)$, and σ_0 is defined by

$$\sigma_0 = \frac{1}{4\beta_a} \left(\frac{\alpha g_\gamma}{\pi f_a}\right)^2 \frac{1}{\sqrt{\epsilon}} L_x L_y L_z^2 B_0^2 \,. \quad (10)$$

Finally, with $B_x(z) = -B_0 \cos(qz)$, the cross section becomes

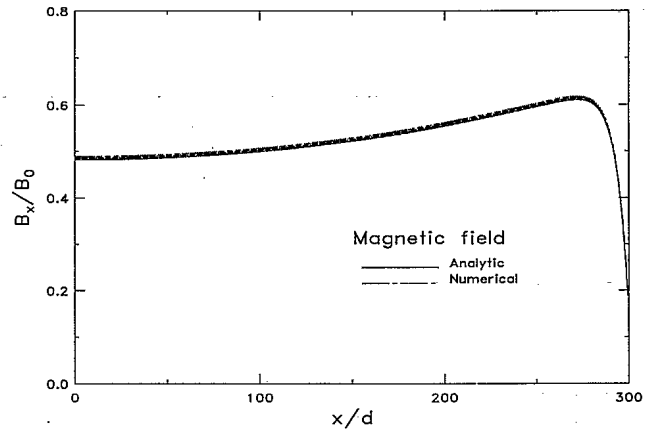

FIG. 2. $B_x(z,x)$ versus x for $|z| = L_z/6$, $I = I_0 \sin(n_z dq)$, $qd = \pi/20$, $L_x = L_z = 600d$. The jagged line is numerical and exact, while the smooth line is the analytical result of Eq. (7).

$$\sigma = \frac{\sigma_0}{L_z^2}\left\{\left(\frac{\sin\{(L_z/2)[E_a(\sqrt{\epsilon}+\beta_{az})-q]\}}{E_a(\sqrt{\epsilon}+\beta_{az})-q}\right)^2 + \left(\frac{\sin\{(L_z/2)[E_a(\sqrt{\epsilon}-\beta_{az})-q]\}}{E_a(\sqrt{\epsilon}-\beta_{az})-q}\right)^2\right\}, \quad (11)$$

where only the resonance terms have been kept. Note that Eqs. (4), (9), and (11) all neglect the effect of the wires in the detector upon the propagation of the electromagnetic field modes. We discuss that effect below.

Because the axion mass is unknown, the detector must be tuned by changing the wave number q of the current configuration. Equation (11) shows that the bandwidth of the detector is $\Delta k_z^d \simeq 2\pi/L_z$. Meanwhile, the width of the axion signal is $\Delta k_z^a \simeq 2\times 10^{-3} m_a$. Provided that the axion signal falls entirely within the bandwidth of the detector ($|q-\sqrt{\epsilon}m_a \pm 10^{-3}m_a| < \pi/L_z$), the power into the detector from resonant $a\to\gamma$ conversion is

$$P = \sigma\beta_a\rho_a = \frac{1}{8}\left(\frac{\alpha g_\gamma}{\pi f_a}\right)^2 V L_z B_0^2 \rho_a \frac{1}{\sqrt{\epsilon}}$$
$$= (2\times 10^{-23}\ \mathrm{W})\left(\frac{VL_z}{(\mathrm{m})^4}\right)\left(\frac{B_0}{8\ \mathrm{T}}\right)^2\left(\frac{m_a}{10^{-4}\ \mathrm{eV}}\right)^2\frac{1}{\sqrt{\epsilon}} \times\left(\frac{\rho_a}{0.5\times 10^{-24}\ \mathrm{g/cm^3}}\right)\left(\frac{g_\gamma}{0.36}\right)^2, \quad (12)$$

where $V = L_x L_y L_z$. This power must be collected and brought to the front end of a microwave receiver. Let ζ be the efficiency with which this can be done and let T_n be the total (physical plus electronic) noise temperature. The signal to noise ratio over the frequency bandwidth $\Delta f_s = 10^{-6} m_a/2\pi$ of the axion signal is

$$\frac{s}{n} = \frac{\zeta P}{T_n}\left(\frac{t}{\Delta f_s}\right)^{1/2}, \quad (13)$$

where t is the measurement integration time. The entire frequency bandwidth of the detector, $\Delta f_d \simeq 1/\sqrt{\epsilon}L_z$, can be examined simultaneously. Thus the search rate for a given signal to noise ratio is

$$\frac{\Delta m_a}{t} = 2\pi\frac{\Delta f_d}{t} = 2\pi\frac{\Delta f_s}{t}\frac{\Delta f_d}{\Delta f_s} = 2\pi\left(\frac{n}{s}\right)^2\left(\frac{\zeta P}{T_n}\right)^2\frac{2\pi Q_a}{m_a L_z}\frac{1}{\sqrt{\epsilon}}$$
$$= \frac{2\times 10^{-7}\ \mathrm{eV}}{\mathrm{yr}}\left(\frac{V^2 L_z}{(\mathrm{m})^7}\right)\left(\frac{B_0}{8\ \mathrm{T}}\right)^4\left(\frac{\rho_a}{0.5\times 10^{-24}\ \mathrm{g/cm^3}}\right)^2\frac{1}{\epsilon^{3/2}} \times\left(\frac{\zeta}{0.3}\right)^2\left(\frac{10\ \mathrm{K}}{T_n}\right)^2\left(\frac{m_a}{10^{-4}\ \mathrm{eV}}\right)^3\left(\frac{4n}{s}\right)^2\left(\frac{g_\gamma}{0.36}\right)^4, \quad (14)$$

where $Q_a = 10^6$ is the "quality factor" of the axion signal, i.e., the ratio of the energy of galactic halo axions to their energy spread.

Taking $T_n \simeq 10$ K as an estimate of the system noise temperature in the $m_a \sim 10^{-4}$ eV$= 2\pi(24.2$ GHz) range, Eq. (14) tells us that a detector of linear dimensions of order three meters is required for a reasonable search rate. At this energy, the wire spacing $d \simeq 2$ mm, so that there will be of order 2×10^6 wires arranged in 2×10^3 planes. A search at smaller axion masses requires larger ($L \sim m_a^{-3/7}$) but less fine grained ($d \sim m_a^{-1}$) detectors. Near $m_a = 10^{-5}$ eV, where T_n will be lower (of order 2 K), the detector needs to be of order 10 m in linear dimension and have 10^5 wires on a $d = 20$ mm grid. In contrast, a search near 10^{-3} eV would need on the order of 10^8 wires on a $d = 0.2$ mm grid.

The electrical current $I(z)$ must be chosen such that its wave number q can be easily tuned. Because $I(z)$ is periodic, the number of different-value currents needed is much smaller than the total number of wires. First, all the wires in a given plane carry the same current and so may be connected in series. Second, the current distribution may be chosen to have odd symmetry about the midplane in the z direction so that for every plane with a particular current $I(n_z)$ there is a symmetry-related one with $-I(n_z)$. Third, the harmonic current function $I(z)$ may be replaced with another periodic function having the same repeat length along z. This would simplify the problem of supplying the current for the detector. We investigated three such current profiles: sine wave, square wave, and triangular wave. The square-wave profile is the simplest, with every wire having the same current magnitude. Figure 3 shows the magnetic field produced by these current configurations as functions of z, given the *same* maximum current strength. The maximum field with a square-wave current profile is about 60% larger than with a sine-wave profile. However, critical current constraints will then require that the current, and hence the field, be reduced by about 20% from what is shown here. In contrast, the current for the triangle-wave profile can be increased slightly, because it is less efficient in generating field than the sine-wave profile. Figure 4 shows the cross section for conversion of axions into photons for the three current profiles. So that each curve is for a detector operating with similar stability margin, the calculations for the square-wave (triangular-wave) profile were done with the value of I_0 decreased (increased) by 20% relative to the sine-wave profile. The cross section shows the expected resonance peak at $m_a = q$ (for $\epsilon = 1$).

The problem of finding the propagating modes of the electromagnetic field in the presence of the regular array of superconducting wires is similar to the problem of

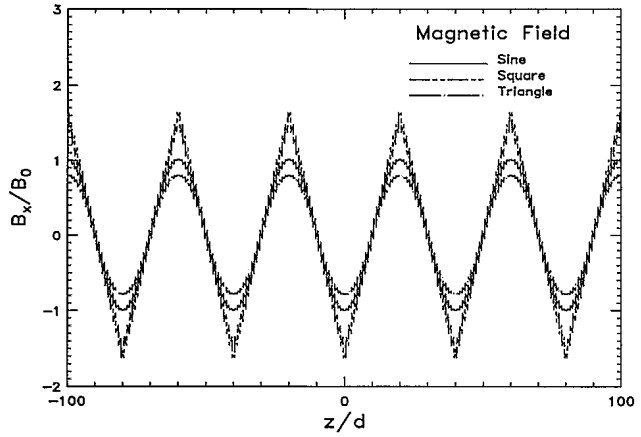

FIG. 3. $B_x(z)$ versus z produced by sine-, square-, and triangular-wave current configurations. $qd = \pi/20$, $L_x = L_z = 500d$.

finding the quantum-mechanical energy eigenstates of a particle in a periodic potential, e.g., an electron in a crystal lattice. Bloch's theorem assures that there are modes of indefinite extent which are periodically varying in each of the three spatial directions. The modes into which axions may convert are those with wave vector $\mathbf{k} \simeq q\hat{\mathbf{z}}$ and with polarization perpendicular to the superconducting wires. Such modes have frequencies $\omega \approx q/\sqrt{\epsilon}$ except near $q = 2\pi/d$ where there is a frequency gap. The size of the gap is related to the size of the wires and may be calculated in perturbation theory. For an actual detector, one must calculate the dispersion relation $\omega(q)$ and the exact electromagnetic propagating modes and modify Eq. (4) accordingly. The important thing to note for the present is that, provided the array of wires can be made sufficiently regular and provided the absorption by the dielectric and by the wires can be neglected, the detector is transparent to the photons from $a \to \gamma$ conversion and hence can be made as large as required to produce a measurable signal.

The wires have small radius r and hence must carry high current density j. A typical upper limit on the current density of presently available multifilamentary NbTi wires is 8000 A/mm^2 [5]. This places an upper limit on the magnetic field since

$$B_0 = \frac{I_0}{qd^2} = \frac{j\pi r^2}{\sqrt{\epsilon} m_a d^2} = (4.8\ \mathrm{T}) \left(\frac{j}{8000\ \mathrm{A/mm}}\right) \left(\frac{r}{\frac{1}{4}d}\right)^2 \left(\frac{10^{-4}\ \mathrm{eV}}{m_a}\right) \frac{1}{\sqrt{\epsilon}} . \quad (15)$$

Equations (14) and (15) indicate that, with presently available superconducting wire technology, the search is feasible up to $m_a \simeq 10^{-4}$ eV but that $m_a \simeq 10^{-3}$ eV would be far more difficult to achieve.

The material in which the wires are embedded must also meet stringent requirements. It must be transparent to microwave radiation, have enough strength to withstand the forces that would move the wires, and have desirable thermal properties in order to contribute to protection of the detector against a quench. Transparent casting resins are reasonable candidates for the embedding material.

The detector design should minimize the number of interconnections between wires, avoid low-temperature mechanical switches, and have the smallest possible number of high-current leads between room temperature and the detector. One possible way of meeting these criteria is to take the array shown in Fig. 1 and deform it into a cylinder, so that the end of the wire $(n_z, -N_x/2)$ which emerges at $y = -L_y/2$ meets the end of the wire $(n_z, -N_x/2 + 1)$ at $y = +L_y/2$, and so on. In this way, the plane of wires at a given n_z becomes a spiral. The spiral could be a NbTi strip etched by photolithographic techniques onto a low-loss insulating sheet. These sheets would then be stacked up to form the body of the detector. Each spiral would be connected to its symmetry-related spiral at $-n_z$ by means of a wire parallel to $\hat{\mathbf{z}}$ that runs down the central region of the cylinder. The two wires that emerge from the rims of the two spirals would then form one circuit of the detector. The circuit would be closed by connecting these wires with a superconducting switch, identical to the persistent-mode switch used in superconducting magnets. If this switch is open, and a second superconducting switch is closed to connect this circuit to the leads from an external supply, the circuit can be energized. Each of the $N_z/2$ circuits could be energized in turn. A bipolar supply would enable either positive or negative values of the current. Thus the energizing circuit would consist of one power supply, one pair of vapor-cooled leads, and N_z superconducting switches.

The detector produces plane-polarized, well-collimated photons which emerge from the ends of the detector in the $\pm\hat{\mathbf{z}}$ direction. The photons can be focused with a parabolic mirror or channeled into a waveguide and brought to the input of a low-noise microwave receiver. The signal consists of thermal and electronic noise along with excess power resulting from axion conversion. As in the case of cavity detectors, the signal will be spectrum analyzed to search for the axion resonance as the detector's operating frequency is swept. The electronics

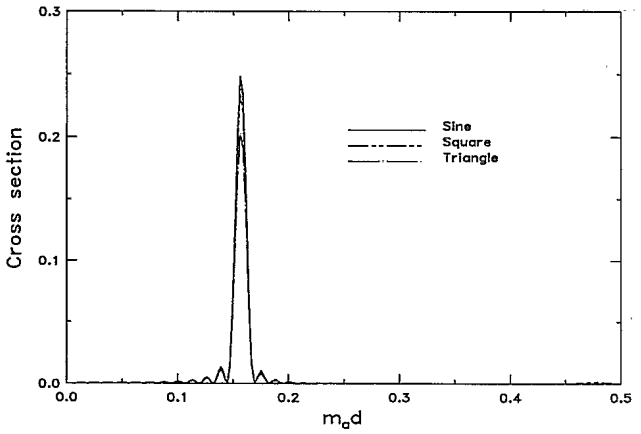

FIG. 4. Conversion cross section of axions into photons as a function of m_a for three current profiles. The current values have been adjusted so that all three cases are equally close to the critical current.

and signal analysis techniques would be similar to those of the cavity detectors.

In summary, we have described a detector for dark-matter axions that could be used to search a part of the allowed range of axion masses that is unreachable in the foreseeable future by cavity detectors.

This work was supported in part by the Department of Energy under Grant No. DE-FG05-86ER40272 at the University of Florida.

[1] Recent reviews include M. Turner, Phys. Rep. **197**, 67 (1990); G. G. Raffelt, *ibid.* **198**, 1 (1990); P. Sikivie, in *The Dark Side of the Universe*, Proceedings of the 17th John Hopkins Workshop on Current Problems in Particle Theory, Budapest, Hungary, 1993, edited by Rita Bernabei and Charling Tao (World Scientific, Singapore, 1994).

[2] P. Sikivie, Phys. Rev. Lett. **51**, 1415 (1983); Phys. Rev. D **32**, 2988 (1985); L. Krauss, J. Moody, F. Wilczek, and D. Morris, Phys. Rev. Lett. **55**, 1797 (1985).

[3] S. DePanfilis *et al.*, Phys. Rev. D **40**, 3153 (1989); C. Hagmann *et al.*, *ibid.* **42**, 1297 (1990); K. Van Bibber *et al.*, "A proposed search for dark matter axions in the 0.6–16 μeV range," LLNL Report No. UCRL-JC-106876, 1991 (unpublished).

[4] Sikivie [2]; P. Sikivie, N. Sullivan, and D. Tanner (unpublished); Sikivie [1].

[5] J. Miller (private communication).